Understanding Rare Earth Elements concentrations, anomalies and fluxes at the river basin scale: The Moselle River (France) as a case study

Pauline Louis, Abdelkrim Messaoudene, Hayfa Jrad, Barakat A Abdoul-Hamid, Davide Anselmo Luigi Vignati, Marie-Noëlle Pons

▶ **To cite this version:**

Pauline Louis, Abdelkrim Messaoudene, Hayfa Jrad, Barakat A Abdoul-Hamid, Davide Anselmo Luigi Vignati, et al.. Understanding Rare Earth Elements concentrations, anomalies and fluxes at the river basin scale: The Moselle River (France) as a case study. Science of the Total Environment, 2020, 742, pp.140619. 10.1016/j.scitotenv.2020.140619 . hal-02897410

HAL Id: hal-02897410

https://hal.univ-lorraine.fr/hal-02897410v1

Submitted on 20 Jul 2020

HAL is a multi-disciplinary open access archive for the deposit and dissemination of scientific research documents, whether they are published or not. The documents may come from teaching and research institutions in France or abroad, or from public or private research centers.

L'archive ouverte pluridisciplinaire **HAL**, est destinée au dépôt et à la diffusion de documents scientifiques de niveau recherche, publiés ou non, émanant des établissements d'enseignement et de recherche français ou étrangers, des laboratoires publics ou privés.

Distributed under a Creative Commons Attribution - NonCommercial - NoDerivatives 4.0 International License

Science of the Total Environment 742 (2020) 140619

Contents lists available at ScienceDirect

Science of the Total Environment

journal homepage: www.elsevier.com/locate/scitotenv

Understanding Rare Earth Elements concentrations, anomalies and fluxes at the river basin scale: The Moselle River (France) as a case study

Pauline Louis [a], Abdelkrim Messaoudene [a], Hayfa Jrad [a], Barakat A. Abdoul-Hamid [a], Davide A.L. Vignati [b], Marie-Noëlle Pons [a,c,*]

[a] Université de Lorraine, CNRS, LRGP, F-54000 Nancy, France
[b] Université de Lorraine, CNRS, LIEC, F-57000 Metz, France
[c] LTSER-Zone Atelier du Bassin de la Moselle, LRGP, 54000 Nancy, France

HIGHLIGHTS

- REEs patterns of headstream waters depend on lithology
- Gd anomaly calculation method influences its numerical value
- The extent of Gd anomalies can be driven by changes in natural Gd levels
- Anthropogenic Gd flux linearly correlates to cumulated population in the watershed
- The ecotoxicological potential of anthropogenic Gd requires further investigation

GRAPHICAL ABSTRACT

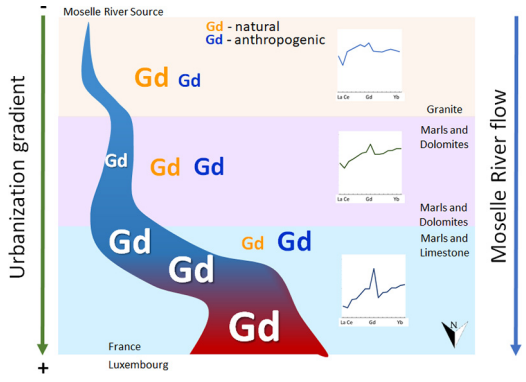

ARTICLE INFO

Article history:
Received 11 May 2020
Received in revised form 26 June 2020
Accepted 28 June 2020
Available online 1 July 2020

Editor: Damia Barcelo

Keywords:
Gadolinium anomaly
Land use gradient
Population gradient
Rare Earth Elements
REEs patterns

ABSTRACT

Anthropogenic activities linked to various new technologies are increasingly disrupting REEs biogeochemical cycles. A catchment-based perspective is therefore necessary to distinguish between natural (i.e., changes in lithology) and human-related sources of REEs variability. In the present study, REEs patterns, anomalies and fluxes were investigated in the French part of the Moselle River basin (Moselle River itself and some of its headstreams and tributaries). The REEs patterns in the headstream waters were highly variable and mostly related to the complex underlying lithology (granite, sandstone, tuff and graywacke). Along the Moselle River, the presence of positive Gd anomalies and a regular LREEs depletion/HREEs enrichment pattern on sandstone/limestone substrates were the most distinctive features. The Gd anomaly varied from 1.8 to 8.7, with anthropogenic Gd representing 45 to 88% of the total Gd. A linear relationship was obtained between the anthropogenic Gd flux and the cumulative population along the watershed. However, the magnitude of the Gd anomalies was shown to depend on the methodological approach chosen for their calculation. The use of a threshold value to identify the presence of an anthropogenic Gd anomaly may therefore be basin (and lithology) dependent, and care has to be taken in comparing results from different rivers or lithologies. Concentration of anthropogenic Gd in the Moselle River and its tributaries were close to, or above, the value of 20 ng/L reported in literature to elicit adverse biological effects in laboratory cell cultures. The ecotoxicological significance of Gd anomalies deserves further investigation because concentrations of anthropogenic Gd may also vary depending on the methodological approach used for calculating Gd anomalies.
© 2020 The Authors. Published by Elsevier B.V. This is an open access article under the CC BY-NC-ND license (http://creativecommons.org/licenses/by-nc-nd/4.0/).

* Corresponding author at: Université de Lorraine, CNRS, LRGP, F-54000 Nancy, France.
E-mail address: marie-noelle.pons@univ-lorraine.fr (M.-N. Pons).

https://doi.org/10.1016/j.scitotenv.2020.140619
0048-9697/© 2020 The Authors. Published by Elsevier B.V. This is an open access article under the CC BY-NC-ND license (http://creativecommons.org/licenses/by-nc-nd/4.0/).

1. Introduction

Rare Earth Elements (REEs) are commonly used in geochemistry as process and/or source tracers, as they behave in a coherent way along the lanthanide series. Many studies have reported changes in their distribution patterns during rock weathering and transport in natural water systems (Elderfield et al., 1990; Sholkovitz, 1992; Tricca et al., 1999; Aubert et al., 2001; Hannigan and Sholkovitz, 2001). In waters unaffected by human activities, negative anomalies of cerium (Ce) and europium (Eu) can occur due to their redox behavior (De Baar et al., 1988; German and Elderfield, 1989; Bau, 1991). Some small gadolinium (Gd) and lanthanum (La) anomalies can also be found in estuaries or seawater because of the differences among REEs complexes stabilities (Byrne and Kim, 1990; Bau, 1999).

However, the worldwide consumption of REEs in new technologies, industries, medicine and agriculture has widely increased over the last decades (Haxel, 2002; Humphries, 2010; Du and Graedel, 2011; Gasanov et al., 2018). These anthropogenic uses disrupt the geochemical and biological cycles of REEs and lead to the enrichment of some REEs in natural waters. Gadolinium enrichment was the first REEs enrichment reported in the 1990s by Bau and Dulski (1996): a positive Gd anomaly due to anthropogenic activities was identified. Since then, Gd anomalies have been documented worldwide and reported in rivers and lakes (Tricca et al., 1999; Möller et al., 2000, 2014; Elbaz-Poulichet et al., 2002; Knappe et al., 2005; Bau et al., 2006; Kulaksız and Bau, 2007; Rabiet et al., 2009; Hissler et al., 2014, 2015, 2016; Klaver et al., 2014; Kim et al., 2020), in groundwater (Möller et al., 2000; Knappe et al., 2005; Rabiet et al., 2009), in estuaries and coastal waters (Nozaki et al., 2000; Elbaz-Poulichet et al., 2002; Kulaksız and Bau, 2007; Lerat-Hardy et al., 2019), and even in tap water (Kulaksız and Bau, 2011a; Tepe et al., 2014; Schmidt et al., 2019).

Indeed, organic Gd complexes are used as a contrast agent in magnetic resonance imaging (MRI). These complexes are water soluble and highly stable to avoid any direct interaction between the toxic Gd^{3+} ion and cellular components during clinical uses. Because of their stability, Gd complexes are not removed by conventional wastewater treatment plants (WWTPs), and WWTP effluents are now recognized as the principal source of anthropogenic Gd (Gd_{anth}) (Bau and Dulski, 1996; Kümmerer and Helmers, 2000; Verplanck et al., 2005, 2010). Toxicological effects linked to the clinical use (via intravenous injection) of Gd-based contrast agents are well established and increased Gd levels have been reported in bones, kidneys, brain, and skin of human subjects following MRI examination, without reported clinical consequences up to now (Chazot et al., 2020). However, the clinical intravenous exposure route has little relevance in environmental contexts and, at the time of writing, we are unaware of reports documenting anomalous Gd levels in humans from drinking water with anthropogenic Gd anomalies. On the other hand, anthropogenic forms of Gd can bioaccumulate in tissues of freshwater bivalves and elicit temporary biochemical responses (Perrat et al., 2017; Pereto et al., 2020). Gadoteric acid, one of the most commonly-used MRI contrast agents and a likely contributor to the observed Gd anomalies, can slow down the growth of a zebrafish cell line at concentrations as low as 20 ng/L (on a Gd-basis), although it does not cause lethal effects at exposures levels up to 200 mg/L (Parant et al., 2019). Estimation of natural vs. anthropogenic concentrations of Gd in natural waters is usually performed after calculating the corresponding Gd anthropogenic anomalies.

The presence of a Gd anomaly is normally estimated using the neighboring REEs of Gd, but currently there is no standardized methodology for this process. Many studies have used Sm and Tb (Bau and Dulski, 1996; Tricca et al., 1999; Knappe et al., 2005; Bau et al., 2006; Klaver et al., 2014) or Eu and Tb (Nozaki et al., 2000; Elbaz-Poulichet et al., 2002). Several more recent publications advise the use of Nd and Sm (Kulaksız and Bau, 2007) or Nd and Eu (Kulaksız and Bau, 2013; Merschel et al., 2015), which are light REEs. Kulaksız and Bau (2007) indicated that the use of light REEs to calculate Gd anomalies leads to Gd* values that are more representative of the background measured in pristine water. On the other hand, Hissler et al. (2015) recommend using Nd and Dy, as they consider Gd a middle REE. Considering that natural REEs abundances and patterns are geologically determined, different methodological choices will not necessarily yield equivalent results in terms of REEs anomalies. The possible influence of such choices on the actual numerical value of a given Gd anomaly must therefore be evaluated to ensure meaningful inter-river comparisons, correct identification of anthropogenic inputs within a given basin and a correct ecotoxicological evaluation of risks related to anthropogenic Gd. Finally, Gd anomalies are increasingly seen as a simple, cheap and easy-to-use proxy for the presence of potentially harmful compounds contained in waste-waters (Pereto et al., 2020; Schmidt et al., 2019), so that inadequate methodological choices may have practical economical and public health implications.

While the Gd anomaly is the most reported one associated with human activities, some studies have highlighted other positive REEs anomalies in natural waters. Kulaksız and Bau (2011b) showed Rhine River contamination by anthropogenic lanthanum from the industrial production of catalysts for petroleum refining. In 2013, analyses conducted on Rhine River surface water samples also revealed a positive samarium anomaly, with the same source as the lanthanum anomaly (Kulaksız and Bau, 2013).

Aquatic ecosystems around large cities, where MRI facilities are numerous, will likely be the most impacted by anthropogenic Gd (Kim et al., 2020; Inoue et al., 2020). However, the pharmacokinetics of contrast agents will also affect their dissemination in a watershed. Urinary excretion of contrast agents by patients having undergone MRI shows an initial rapid elimination phase (half-time of about 2 h) followed by a slower release with a half-time about 6 days (Czoch, 2019). However, Kümmerer and Helmers (2000) reported the detection of contrast agents in patients' urine 39 days after injection. It is therefore likely that anthropogenic Gd might be disseminated in large watersheds depending upon the population density and the distribution of urban areas.

Therefore, the first purpose of the present study is to investigate the relation between REEs distribution vs. landuse and population in a complex watershed. We have selected the French part of the Moselle River watershed, including headstreams in the Vosges Mountains, tributaries and the Moselle River itself from its source to the Luxembourg border. To the best of our knowledge, there has not been any REEs investigation conducted in the Moselle River basin at this scale. Only some data about REEs in the headstreams in the Vosges Mountains are available (Tricca et al., 1999; Aubert et al., 2001, 2002; Stille et al., 2006). The French Moselle River catchment is of great interest because of its geological and land occupation contrasts. The second focus of this study is to compare the effect of different calculation methods on the numerical value of the observed Gd anomalies. The third objective is to evaluate whether the measured concentrations of REE, including anthropogenic vs. natural Gd, may be of ecotoxicological concern at the basin level.

2. Materials and methods

2.1. Studied area: the Moselle River catchment

The Moselle River is one of the main Rhine River tributaries. Its French part (314 km length) is located in northeastern France, with its source in the Vosges Mountains (Bussang) and a catchment area of 11,437 km^2 (Fig. 1, with enlargements of the upstream and middle sections in Figs. SM1 and SM2 of Supplementary Materials). The studied area is limited to the French part of the Moselle River watershed, from its source to the Luxembourg border. All distances, given in river km (rkm), are calculated with respect to the source. Samples were also collected in the Vosges mountains headstreams (upstream of any known anthropogenic activity) and in twelve Moselle River tributaries (from south to north): the Moselotte River (Mo), Cleurie River (Cl), Vologne

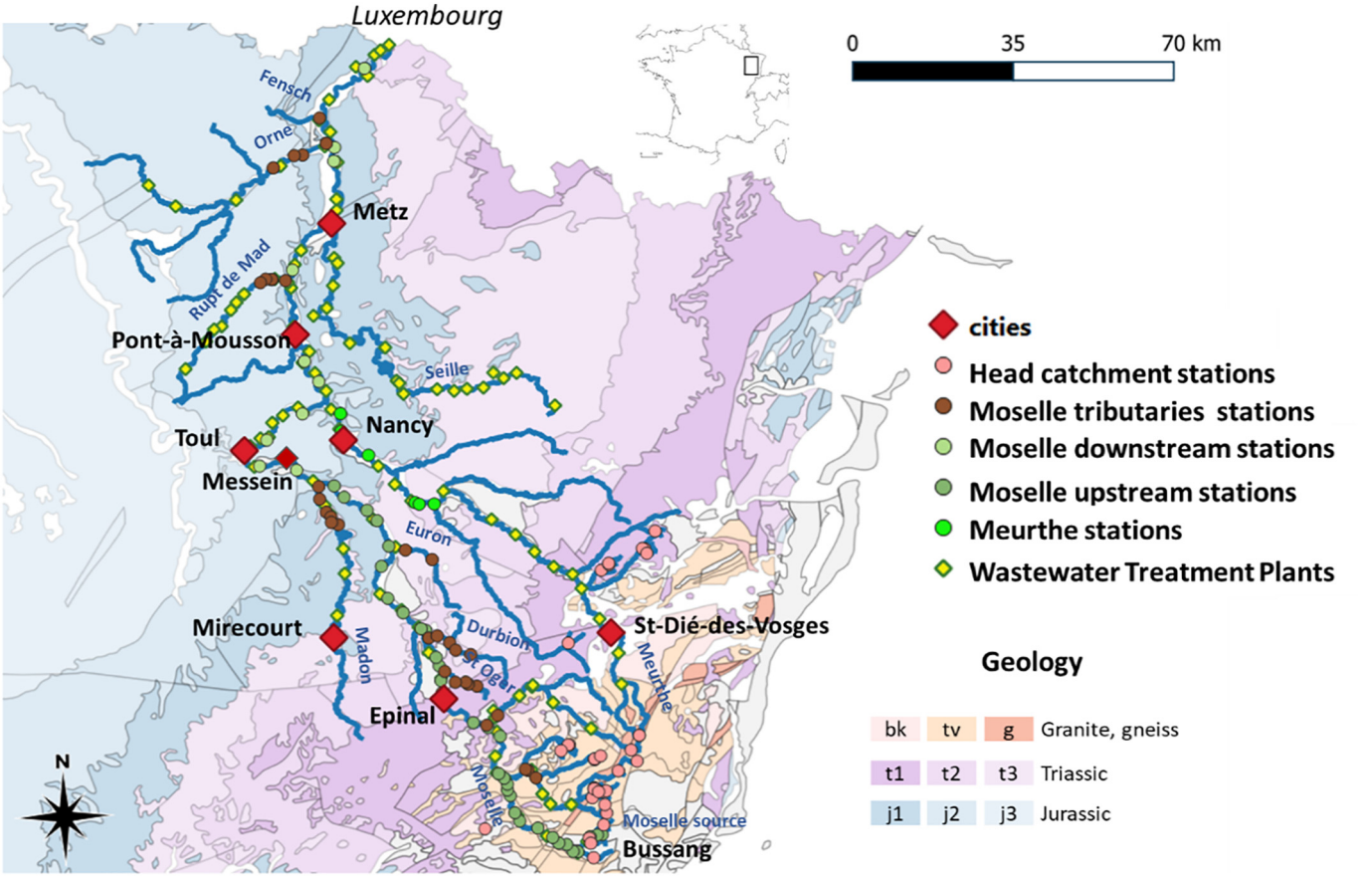

Fig. 1. The French part of the Moselle basin, with its main tributaries, cities, WWTPs, and simplified geological characteristics. g = granite; tv = Tournasian/Visean, bk = Cambrian; t1, t2 and t3 = Lower, Middle and Upper Triassic periods, respectively; j1, j2 and j3 = Lower, Middle and Upper Jurassic periods, respectively.

River (Vo), Saint-Oger River (SO), Durbion River (Du), Euron River (Eur), Madon River (Ma), Meurthe River (Me), Seille River (Sei), Fensch River (Fen), Rupt de Mad River (RdM) and Orne River (Or) (Fig. 1).

Information on the geology was obtained from the InfoTerre database (http://infoterre.brgm.fr). The land use analysis was based on 2018 CORINE Landcover data (https://www.data.gouv.fr/fr/datasets/corine-land-cover-occupation-des-sols-en-france/), and the population analysis was based on the 2017 legal census (https://www.insee.fr), by taking all communities along the Moselle and its main tributaries and subtributaries into account (see Table SM1in Supplementary Materials). It was assumed that the communities along the rivers were the most likely to contribute to its pollution. The location of the wastewater treatment plants was obtained from the SIERM website (http://rhin-meuse.eaufrance.fr/).

From a geographical, geological and land use point of view, the studied catchment can be divided into thREEs parts (Figs. SM3 and SM4 of the Supplementary Materials). The Vosges Mountains constitute the first part, from the Moselle River source to Epinal (rkm 72.2 km), with mostly crystalline rocks (granites, graywackes, gneisses) and some sedimentary rocks (sandstones such as Buntsandstein) (Nédeltcheva et al., 2006a, 2006b). Land use in this area is mostly devoted to forestry (75%) and agriculture (20%) (cattle breeding). The Lorraine Plateau is the second part, from Epinal to Messein (rkm 144), with sedimentary rocks from the Trias period (marls, dolomites, gypsum, belonging to the Muschelkalk and Keuper formations). This part is characterized by a reduction in the forested areas (55%), an increase in agricultural land (35%) and some industrial zones around the main cities. The Moselle cuestas constitute the last part, from Messein to the Luxembourg border (rkm 314), with sedimentary rocks from the Jurassic period (marls, limestone, clays). In this part, past and present industrialization is more developed than in the other areas of the basin (up to 11%) and includes the two main cities of the catchment, Nancy (105,000 inhabitants) and Metz (115,00 inhabitants, rkm 250), and their urban areas (256,000 inhabitants for Grand Nancy and 222,000 for Metz Métropole). The areas occupied by forestry and agricultural activities are equivalent (44% each). The most important industries in the Moselle River watershed are related to wood (sawmills, papermills), textile (upstream of Messein) and to sodium chloride extraction and sodium carbonate production (along the Meurthe River, 20 km upstream of its junction with the Moselle River i.e. rkm 195). Some large metal-related industries are remaining: pig-iron mill in Pont-à-Mousson (rkm 215) and steel mills in the Fensch River valley, which joins the Moselle River at rkm 275, close to the Luxembourg border. Except steel-mills, none of these industries is known to use REEs. Grand Nancy exclusively uses Moselle River water for drinking water production: the intake station is located at Messein. Metz Métropole combines surface water (Rupt de Mad River) and Moselle River alluvial groundwater for its drinking water. The Grand Nancy WWTP discharges into the Meurthe River, just upstream of its junction with the Moselle River, and the Metz Métropole WWTP discharges directly into the Moselle River.

2.2. Sampling

A snapshot sampling strategy was applied, meaning that all the samples were collected in a reduced time window (10 days). All the samplings occurred in a period of median flow, within a coefficient of variation of 20% observed for all the 12 gauging stations in operation along the Moselle River in April 2019 (http://www.hydro.eaufrance.fr/). Sampling campaigns were conducted in April 2019 and were divided into four groups: the headstreams (April 2, 2019; 31 stations), the upstream section of the Moselle River from the source to Messein (April 12, 2019; 28 stations), the downstream section of the Moselle River

from Messein to the Luxembourg border (April 04, 2019; 15 stations) and the main tributaries (April 5 and 11, 2019; 29 stations). The geographical position of each station, sampled once, is given in the Tables SM2 to SM4 of the Supplementary Materials. Except for the headstreams, safe bridges with pedestrian access were selected from maps (https://www.geoportail.gouv.fr/) to serve as sampling stations. The average distance between sampling station along the upstream section of the Moselle River was 4.6 km. It was higher for the downstream section (15 km), as less safe bridges were available. For the tributaries, a limited number of stations was selected based on the presence of safe bridges sufficiently close to their junctions with the Moselle River.

Surface water samples were collected in 500 mL PTFE bottles previously washed with HNO_3 acid and rinsed with ultrapure water. Except for headstreams, where the bottles were directly immersed in the water, these samples were taken using a bailer thrown into the river from the middle of a bridge (sampling depth = 5 cm). Bottles were rinsed with river water before sample collection. One bottle was used at each sampling station to measure all the parameters. The samples were stored at 4 °C and filtered within 24 h after sampling.

2.3. Analytical methods

The samples were filtered in the laboratory through 0.45 μm nominal pore size regenerated cellulose syringe filters (Phenomenex®). For the rest of this paper, the fraction below 0.45 μm is called the "filterable fraction" and consists of dissolved ions and colloids <0.45 μm. Aliquots (50 mL for REEs and minor elements, 10 mL for major elements) of the filterable fraction were acidified immediately after filtration with ultrapure HNO_3 acid (at 1% *v*/v, acid class "Optima" to determine REEs and minor elements; and at 2% v/v, acid class "Trace mMetal" for major cations). Other sample aliquots (80 mL) were preserved at 4 °C without acidification for measurements of dissolved organic and inorganic carbon (DOC and DIC), total nitrogen (TN), major anions, orthophosphates, and ammonium.

DOC and DIC were measured with a Shimadzu TOC VCHS combined with a TNM-1 module for TN determination. Orthophosphates and ammonium were quantified by spectrophotometric methods with a HACH DR 2400 spectrophotometer (HACH PhosVer3 detection method 8048 for orthophosphates and Nessler micromethod adapted from HACH method 8038). Major anions (Cl^-, SO_4^{2-}, NO_3^-, NO_2^-) were determined by ion chromatography (Thermo Scientific Dionex iCS 3000), and major cations (Mg, Na, K, and Ca) were determined by inductively coupled plasma atomic emission (ICP AES) (Thermo Scientific iCAP 6300 Duo).

REEs were determined using Inductively Coupled Plasma Mass Spectrometry (ICP-MS) (Thermo Scientific iCAPQ+prepFast) without preconcentration. Re and Rh at 50 ppb were used as online internal standards. The instrument was tuned for oxide and doubly charged ion formation, and interference corrections for oxide and hydroxide were applied when necessary. The analytical error was below 5%.The quantification limit, calculated as 10 times the standard deviation of replicated blank measurements, was 1 ng/L for all REEs. The filtration blank results ($n = 15$) were always below detection limits. SLRS-6 reference material water was used to control the ICP-MS accuracy and reproducibility (Yeghicheyan et al., 2019) (Table SM5 of the Supplementary Materials).

2.4. Calculations

The REEs concentrations were normalized by the Post Archean Australian Shale (PAAS) (McLennan, 1989). The Ce and Eu anomalies, which are mostly natural anomalies in the hydrosphere, were calculated using Eq. (1) (Hissler et al., 2015) and Eq. (2) (Olivarez and Owen, 1991), respectively.

$$Ce/Ce^* = Ce_{PAAS}/(0.5 \times La_{PAAS} + 0.5 \times Pr_{PAAS}) \quad (1)$$

$$Eu/Eu^* = Eu_{PAAS}/\left(Sm_{PAAS}{}^{0.67} \times Tb_{PAAS}{}^{0.33}\right) \quad (2)$$

The Gd anthropogenic anomaly and the corresponding anthropogenic and natural Gd concentrations were calculated with several approaches. In the remainder of the paper, the results for Gd/Gd* and Gd_{anth} will be discussed based on the Nd and Dy calculations, but a comparison between different methods (see below) will also be presented.

(According to Bau and Dulski, 1996)

$$Gd/Gd^* = Gd_{PAAS}/(0.33 \times Sm_{PAAS} + 0.67 \times Tb_{PAAS}) \quad (3)$$

(According to Kulaksız and Bau, 2007)

$$Gd/Gd^* = Gd_{PAAS}/10^{(2\times \log Sm_{PAAS} - log Nd_{PAAS})} \quad (4)$$

(According to Kulaksız and Bau, 2013),

$$\log Gd^* = (4 \times \log Eu_{PAAS} - \log Nd_{PAAS})/3 \quad (5)$$

(According to Hissler et al., 2015),

$$Gd/Gd^* = Gd_{PAAS}/(0.4 \times Nd_{PAAS} + 0.6 \times Dy_{PAAS}) \quad (6)$$

$$Gd_{anth} = Gd - Gd^* \quad (7)$$

In these equations, X is the measured concentration in the samples, X* is the calculated geogenic concentration, and X_{PAAS} is the elemental concentrations measured in the sample and normalized to the PAAS.

Fractionation between light REEs (LREEs; La, Ce, Pr, Nd) and heavy REEs (HREEs; Dy, Ho, Er, Tm, Yb, Lu) was calculated using the PAAS-normalized La_{PAAS}/Yb_{PAAS} ratio, that between LREEs and middle REEs (MREEs; Sm, Eu, Gd, Tb) was calculated using the La_{PAAS}/Sm_{PAAS} ratio, and that between MREEs and HREEs was calculated using the Gd_{PAAS}/Yb_{PAAS} ratio. All the necessary flow data to estimate REEs fluxes were obtained from the HYDRO database (http://www.hydro.eaufrance.fr/).

3. Results and discussion

3.1. Surface water main characteristics

This section summarizes the surface water main characteristics (DOC, DIC, NO_3^-, NH_4^+) along the Moselle River, as they provide information about the geological substrate and/or anthropogenic pressure. The related figures can be found in the Supplementary Materials (Fig. SM5). The inorganic carbon describes the carbonate and bicarbonate species and shows clear changes in geology along the Moselle River. The DIC is approximately 4.7 mg/L at the Moselle River source and ranges from 2.3 to 3.6 between Bussang (rkm 3.1 km) and Arches (rkm 62.3). From downstream of Epinal (rkm 71.2) up to Messein (rkm 144), the DIC varies from 3.7 to 12.9 mg/L due to the transition between granitic rocks and marls/dolomites. Downstream of Messein, the DIC increases up to 36.3 mg/L at Malling (rkm 293) close to the border with Luxembourg. Dissolved organic carbon, nitrates and ammonium are parameters related to urbanization and anthropogenic activities (Henze et al., 2002). The DOC concentration at the Moselle River source is 0.4 mg/L and remains lower than 1.4 mg/L until Eloyes (rkm 53.3 km). This area corresponds to a rather sparsely populated zone, with a population density of 130 inhabitants/km^2, to be compared to the average value of 320 inhabitants/km^2 along the Moselle River (calculated between the source and the Luxembourg border). Downstream of Eloyes, industrialization withpaper mills at Arches (rkm 62.3 km) and Golbey (rkm 78 km) and urbanization cause an increase in DOC concentration from 1.9 to 3.3 mg/L.

Nitrates can be introduced into aquatic systems in different ways: via atmospheric emissions (Driscoll et al., 2001), fertilizer run-off (Deal et al., 1986), and WWTP effluents (Henze et al., 2002). Nitrates are approximately 1.1 mgNO_3^-/L at the Moselle River source and

increase with the population up to 14 mgNO_3^-/L at the Luxembourg border. The ammonium concentration stays very low (0.02 to 0.10 mgNH_4^+/L) or lower than the quantification limit from the source to Arches (rkm 62.3), except for the sample "Les Meix" (29.9 rkm; 0.65 mgNH_4^+/L), which is just downstream of a WWTP discharge. The ammonium concentration from Arches (rkm 62.3) to Messein (rkm 144 km) varies between 0.06 and 0.21 mgNH_4^+/L and increases to 0.31 mgNH_4^+/L downstream of Messein and to 0.70 at Millery (rkm 202 km). Millery is the sampling point just downstream of the confluence between the Moselle River and the Meurthe River. The Meurthe River receives the WWTP effluents of Grand Nancy and has salt industries that use ammonia in their operation along its course (Steinhauser, 2008).

3.2. REEs concentrations and patterns

3.2.1. Head catchments

Depending on the geological substrate and anthropogenic pressure, the REEs patterns in the Vosges headstreams can be divided into thREEs groups. The first group represents water in contact with tuff and greywacke (Fig. 2a). In this part of the Vosges Mountains, the total REEs concentration ranges between 34 and 232 ng/L, with LREEs representing 58 to 68% of the total REEs, MREEs representing 9 to 26%, and HREEs representing 7 to 19%. The patterns of these samples present a strong negative Ce anomaly (Ce/Ce*: from 0.15 to 0.44) and La_{PAAS}/Yb_{PAAS} ratios from 0.19 to 0.38, indicating slight LREEs depletion. The second group represents water in contact with sandstone (Fig. 2b). In this group, the total REEs concentration varies between 109 and 1150 ng/L, with LREEs representing 53 to 64% of total REEs, MREEs representing 14 to 17%, and HREEs representing 18 to 30%. REEs patterns show a negative Ce anomaly (Ce/Ce*: from 0.41 to 0.74) and a small positive Eu anomaly (Eu/Eu*: from 1.25 to 1.48). La_{PAAS}/Yb_{PAAS} values vary from 0.14 to 0.20, indicating slight LREEs depletion and HREEs enrichment. The third group represents water in contact with granites (Fig. 2c and d). In this part, the total REEs concentration ranges between 324 and 1395 ng/L, with LREEs representing 67 to 86% of the total REEs, MREEs representing 9 to 17%, and HREEs representing 5 to 15%. The REEs patterns present a slight concavity, with depletion in LREEs (La_{PAAS}/Sm_{PAAS}: from 0.24 to 0.53) and HREEs (Gd_{PAAS}/Yb_{PAAS}: from 1.20 to 1.81). Leybourne et al. (2000) explain that this kind of concave pattern could be produced by mineral weathering of host rocks, particularly phosphate-bearing minerals. Furthermore, other studies of REEs in Vosges mountain streams on granitic substrates (Tricca et al., 1999; Aubert et al., 2001) exhibit similar PAAS-normalized REEs patterns. Granitic background water patterns do not show a negative Ce anomaly or show only a small anomaly (Ce/Ce*: from 0.57 to 1.05), and some of them display a slight negative Eu anomaly (Fig. 2d) ranging from 0.50 to 0.93. According to Tricca et al. (1999), this Eu anomaly is strongly lithology dependent.

None of these patterns in head catchment streams reveals a positive Gd anomaly, except for the sample "Lamerey", collected at the junction of the stream with the Moselle River (rkm 3.5 km), which presents a small Gd anomaly of 2.9 (based on Eq. (6)).

3.2.2. The Moselle River

From the Moselle River source to the Luxembourg border, REEs patterns can be split into thREEs groups (Fig. 3a, b and c), depending on the geological substrate and urbanization. In the Vosges Mountains part, from the source to Epinal (rkm 71.2), the total REEs concentration fluctuates between 173 and 315 ng/L, with a very low concentration of 33 ng/L at the source. LREEs represent 68 to 78% of the total REEs, MREEs represent 14 to 20%, HREEs represent 7 to 11%, and [Gd] represents 4 to 7%. These REEs parameters do not show any specific trend in this part of the Moselle River. The surface waters of the Lorraine Plateau, from Epinal to Messein (rkm 144), have a total REEs concentration ranging from 205 to 487 ng/L, with the concentration decreasing from upstream to downstream. LREEs represent 68 to 73% of the total REEs, MREEs represent 15 to 17%, HREEs represent 10 to 14%, and [Gd] represents 6 to 9%. The percentages of LREEs and Gd (%LREEs and %Gd) globally decrease from upstream to downstream, while there is no clear trend for %MREEs and %HREEs. From Messein to the Luxembourg border, the total REEs concentration ranges between 74 and 206 ng/L, decreasing from upstream to downstream. LREEs represent 51 to 69% of the total REEs, MREEs represent 16 to 36%, HREEs represent 13 to 16%, and [Gd] represents 8 to 28%. From upstream to downstream, %LREEs decreases while %MREEs increases. This increase can be related to the increase in %Gd from 51 to 82% of the MREEs. For %HREEs, no clear trend emerges.

All patterns of the Moselle River display a natural negative Ce anomaly. This anomaly is more important upstream of Epinal (mostly gneiss, granite, and sandstone background, with sparse urbanization), from 0.15 to 0.57, than downstream of Epinal (mainly marls, dolomites and limestone background, with larger urbanization), from 0.60 to 0.87. The REEs patterns of the Moselle River from Bussang to Epinal exhibit MREEs enrichment. Fig. 3b and c, corresponding to the Moselle River between Epinal and Messein (marls and dolomites from the Trias period) and the Moselle River between Messein and the border (limestone and marls from the Jurassic period), respectively, show LREEs depletion and HREEs enrichment. These depletions and enrichments increase along the river flow, with the La_{PAAS}/Yb_{PAAS} ratio varying from 0.48 (Epinal) to 0.19 (Mailing, last point before the Luxembourg border) (Fig. 4). The decrease in La_{PAAS}/Yb_{PAAS} could be explained by geochemical effects. Sholkovitz (1995) demonstrated that the order of REEs adsorption onto particle surfaces upon increasing pH is LREEs> MREEs> HREEs. Along the Moselle River, pH values vary from 6 to 6.5 in the Vosges Mountains section (La_{PAAS}/Yb_{PAAS} 0.38–0.78), from 7 to 7.5 between Epinal and Messein (La_{PAAS}/Yb_{PAAS}: 0.26–0.34), and from 8 to 8.5 up to the Luxembourg border (La_{PAAS}/Yb_{PAAS} 0.15–0.27). Moreover, the solubility of HREEs is enhanced by carbonate speciation, producing LREE-depleted REEs patterns in waters where REEs are complexed by carbonate or bicarbonate species (Byrne and Kim, 1990; Johannesson and Lyons, 1994; Leybourne et al., 2000). Dissolved inorganic carbon increases from the source to the Luxembourg border, especially downstream of Epinal, where the geological substrate changes from granite to sandstone and then limestone. A significant negative linear relationship (significance level $\alpha = 0.05$, coefficient of determination = 0.77) was found between La_{PAAS}/Yb_{PAAS} and DIC along the Epinal-Malling stretch. The pH and inorganic carbon variations along the Moselle River influence the REEs distribution in the dissolved water column.

Another explanation is that the decrease in the La_{PAAS}/Yb_{PAAS} ratio could have an anthropogenic origin. Hissler et al. (2014, 2016) proposed that this LREEs-depleted pattern might result from WWTP effluent discharge onto rivers under "normal" river flow conditions (except flood events). Indeed, WWTP effluents have a very low La_{PAAS}/Yb_{PAAS} ratio (e.g., 0.02–0.07; (Hissler et al., 2016, 2014)) compared to values observed in river waters. Regarding the positive Gd anomaly, it is detectable from sampling point "Le Pont Jean" (rkm 9.5) with a value of 1.8 and reaches a value of 8.7 near the Luxembourg border (using Dy- and Nd-based calculations).

3.2.3. The Moselle River tributaries

Fig. 5 represents REEs normalized patterns of the Moselle River's tributaries. The REEs patterns are split into four subfigures according to where tributaries flow into the Moselle River. All the REEs patterns display a negative Ce anomaly, except those of Saint-Oger (Ce/Ce*: 0.94–1.05). Negative cerium anomalies are more important for tributaries flowing into the Moselle River upstream of Epinal and going through granite/sandstone substrates (Ce/Ce*: 0.45–0.57) (Fig. 5a) than for other rivers (Ce/Ce*: 0.65–0.84). The REEs patterns presented in Fig. 5a show a small negative europium anomaly (Eu/Eu*: 0.81–0.95) and slight MREEs enrichment. These characteristics could be related to the REEs patterns of headstreams (Fig. 2c and d). Indeed, the Moselotte River and Cleurie River flow on a granitic background. The Vologne

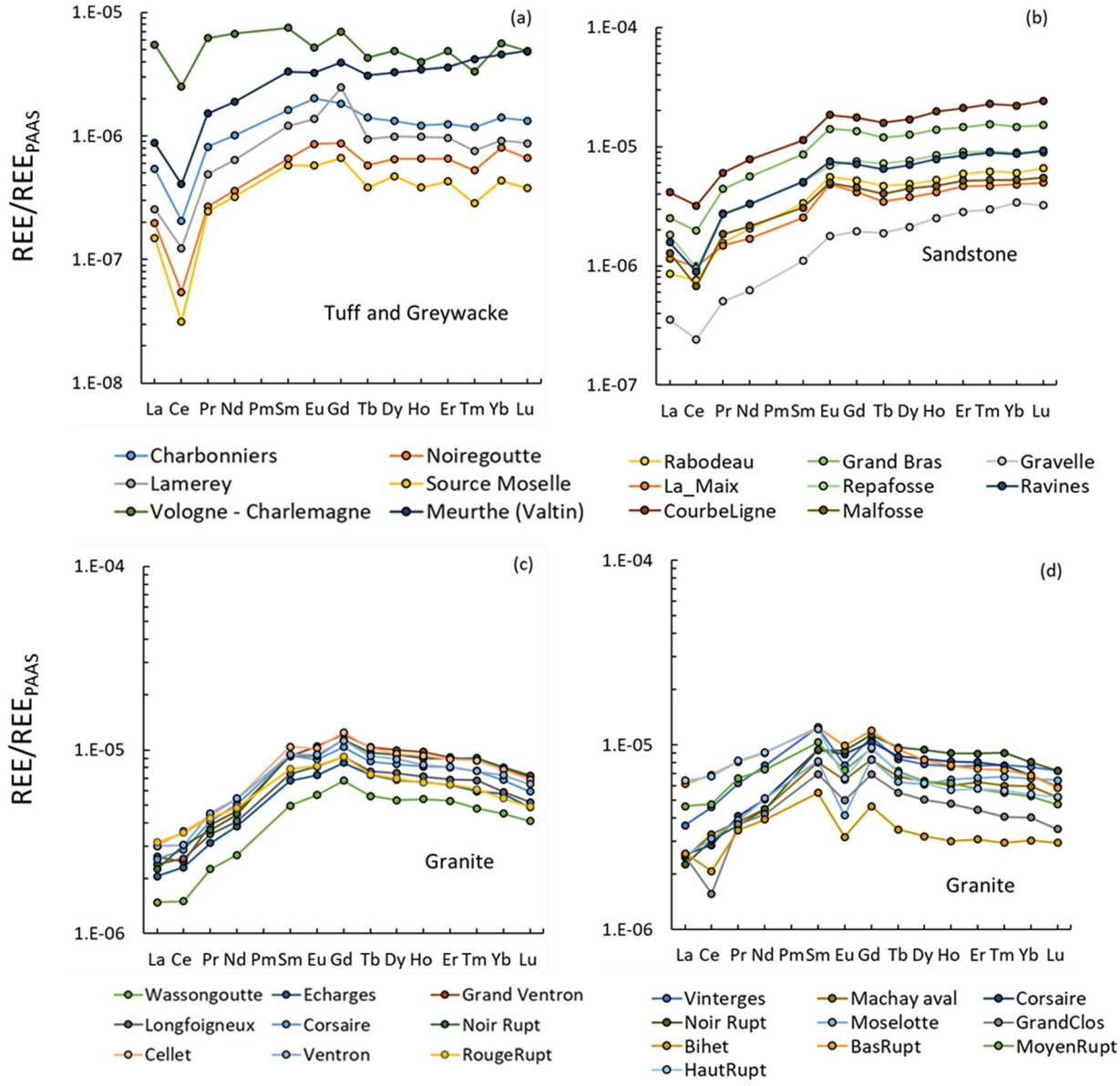

Fig. 2. Headstream REEs patterns, normalized with respect to PAAS, in the Vosges Mountains: waters in contact (a) with tuff and graywacke, (b) with sandstone, (c) and (d) with granite. REEs are in abscissa.

River source is on a granitic background, but sandstone soils are present further downstream. Some REEs patterns of Durbion and Saint-Oger (Fig. 5b) present slight MREEs enrichment. Those rivers have sources on sandstone backgrounds, but downstream, these rivers flow on Muschelkalk formations. The tributaries of the Moselle River downstream of Nancy (Fig. 5c) flow on marls/limestone and their REEs patterns display LREEs depletion and HREEs enrichment (La_{PAAS}/Yb_{PAAS} ratio: 0.19–0.36) as observed, for example, in the Moselle River sample locations downstream of Messein. A positive gadolinium anomaly is visible in the REEs patterns of the Madon River (Ma), Meurthe River (Me), Rupt-de-Mad River (RdM), Seille River (Se) and Fensch River (Fe), with values ranging from 1.9 to 12.7 (using Dy- and Nd-based calculations).

3.3. Gd anomaly calculations

Although reporting of anthropogenic Gd anomalies in natural waters continues to increase, a standardized method to identify such anomalies has not yet been defined. Using our set of data for the Moselle River sampling stations, we calculated the Gd anomaly using different known equations (Eqs. (3) to (6)). The results of these calculations are presented in Table 1 together with calculations of Gd* and Gd_{anth} obtained from Gd/Gd* calculated using Eq. (6). The different equations do not give the same value of Gd/Gd*, with the use of Nd and Dy (Eq. (6)) tending to maximize the anomaly and the use of Sm and Nd (Eq. (4)) tending to minimize it. Eqs. (4) and (5) give the smallest values of the Gd anomaly, in agreement with Kulaksız and Bau's (2007) assertion on the use of LREEs in Gd/Gd* calculations. However, all four equations sort Gd anomalies in the same order, i.e., the smallest Gd anomaly is always obtained for the same sample irrespective of the calculation method. It is therefore possible to compare the intensities of Gd anomalies among samples only if the anomaly is calculated in the same way for all samples. Furthermore, caution must be exercised to set a threshold value to classify a given Gd anomaly as anthropogenic. Using Sm and Tb (Eq. (3)) to calculate Gd/Gd*, Bau et al. (2006) defined a value of 1.5 as the threshold for an anthropogenic Gd anomaly. Applying this value to the present data for the Moselle River would imply the presence of anthropogenic Gd at the Moselle River source (Gd/Gd* = 1.6 using the Nd and Dy method; Table 1), which is not consistent with the known geochemical conditions. Moreover, if we draw a parallel between the values in Table 1 and the REEs patterns in Fig. 3a, the Gd

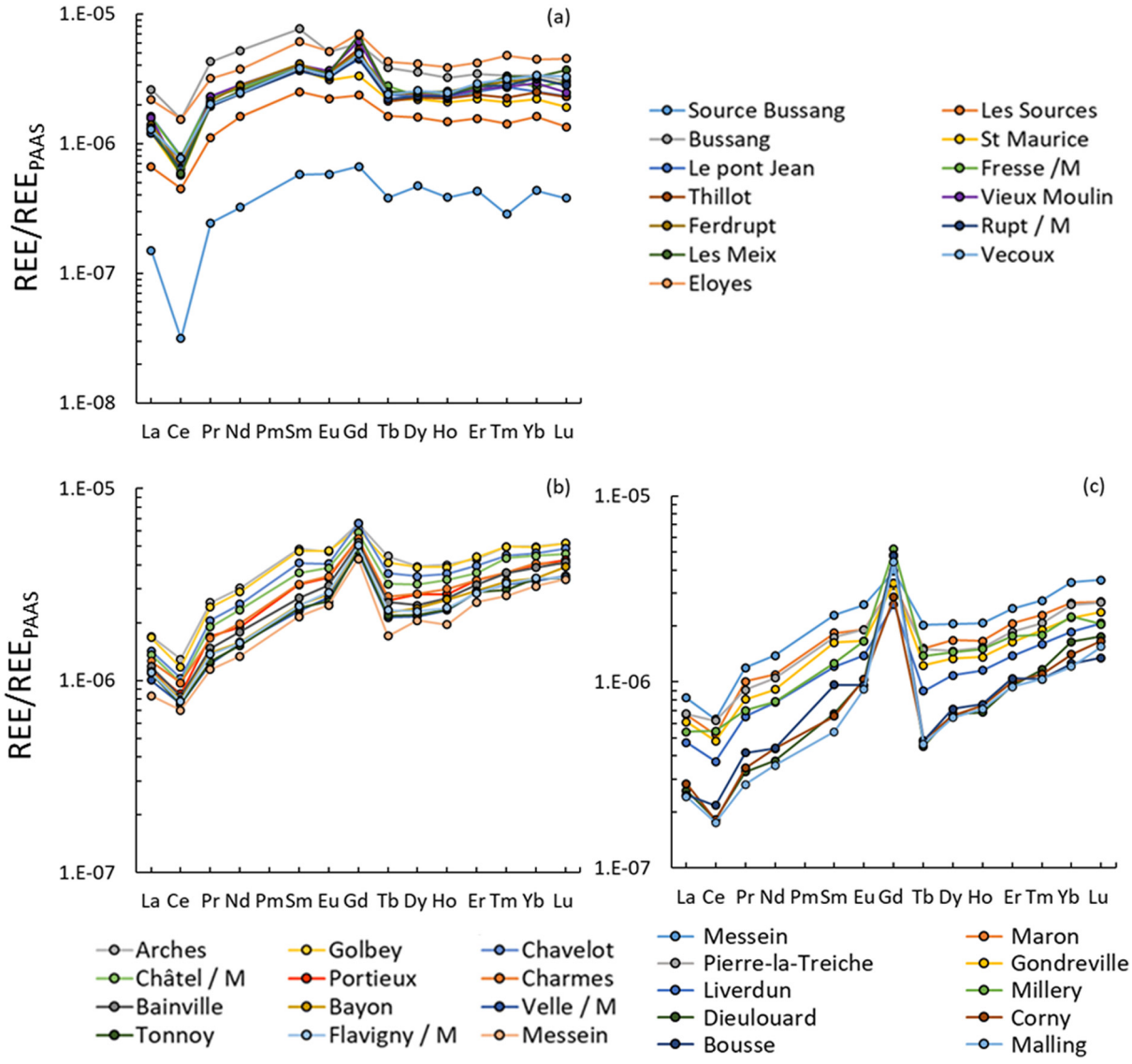

Fig. 3. Moselle River REEs patterns, normalized with respect to PAAS, (a) in the Vosges Mountains part, from the Bussang source to Epinal, (b) along the Lorraine Plateau, from Epinal to Messein, and (c) along the Moselle cuestas, from Messein to the Luxembourg border. REEs in abscissa.

anomaly appears clearly at the "Le Pont Jean" sample, which also corresponds to a Gd anomaly of 1.6 using Sm and Tb. This is why it was decided to take 1.8 as the threshold value here, using Nd and Dy for calculation. It should be noted that the use of Nd and Dy in the Gd anomaly calculation will increase the Gd_{anth} concentration and $\%Gd_{anth}$ over those determined with other calculations.

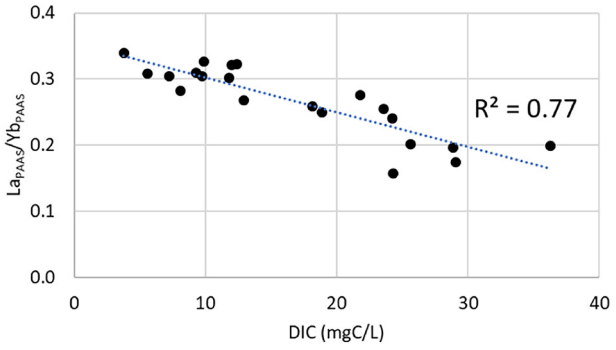

Fig. 4. Relation between LA_{PAAS}/Yb_{PAAS} and DIC in Moselle River waters for the stretch between Epinal and Malling.

In the head catchment, only one sample ("Lamerey") shows a Gd anomaly of 2.9. In this sample, Gd_{anth} represents 65% of the total Gd (Gd_{tot} 11 ng/L). Unlike other headstream samples that were taken in nonurbanized areas, the "Lamerey" sample was collected in a small village (Bussang) where mixed sewage treatment (collective and noncollective) is taking place. This small Gd anomaly can then be explained by the presence of noncollective sanitation units, which can release effluent contaminated by Gd in the environment. Gd can be released for at least one month after MRI examination (Kümmerer and Helmers, 2000). Along the Moselle River course, a positive Gd anomaly appears from the "Le Pont Jean" sampling point (rkm 9.5) (Fig. 2a) with a small value of 1.8 (Table 1). The positive Gd anomaly remains detectable in all water samples along the Moselle River after the "Le Pont Jean" sampling point, increasing to a value of 8.7 near the Luxembourg border. The Gd_{anth} proportion in the filterable fraction varies from 44% to 88% of the total Gd. The increase in the positive Gd anomaly can be related to the increase in the cumulative population along the Moselle River. The two steps at the "Millery" (rkm 202) (Gd/Gd*: 4.4) and "Ay" (rkm 266) (Gd/Gd*: 7.6) stations correspond to WWTP discharges from the Nancy (500,000 person equivalent) and Metz (440,000 person equivalent) urban areas, respectively. Alternatively, it is also noteworthy that natural Gd levels, estimated using

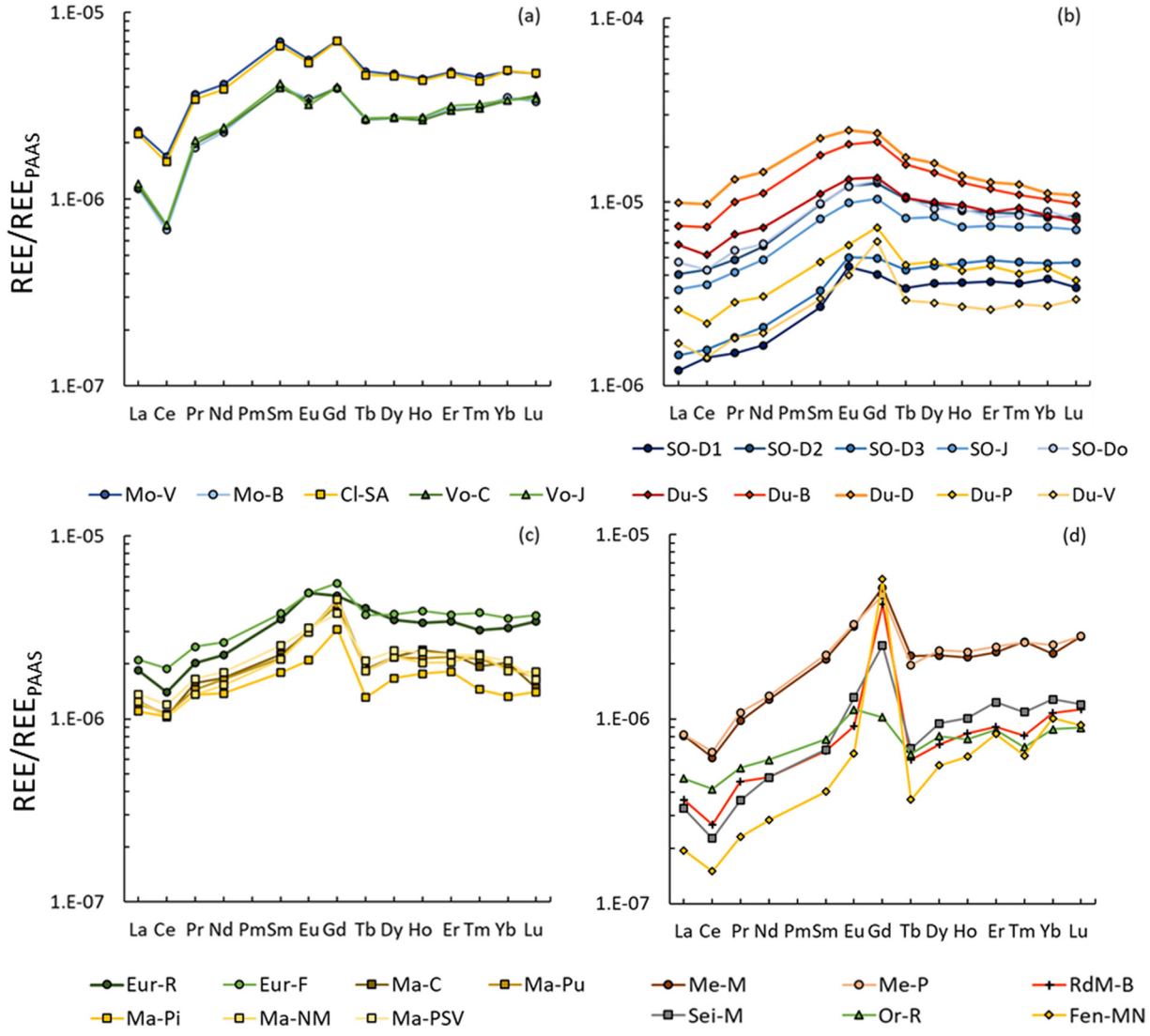

Fig. 5. Tributary REEs patterns, normalized with respect to PAAS, according to where they flow into the Moselle River, (a) upstream of Epinal, (b) and (c) between Epinal and Messein, (d) downstream of Messein. REEs in abscissa.

Eqs. (6) and (7), showed a decreasing tendency along the Moselle River starting from Eloyes (rkm 53.3). Thus, variation in a positive Gd anomaly can be driven by both an actual increase in anthropogenic Gd inputs or by a decrease in natural Gd levels at constant concentrations of anthropogenic Gd. Considering the corresponding ranges in the Moselle river (2.5–18.5 ng/L for Gd* and 9.3–20.3 ng/L for Gd_{anth}), the second factor seems to be the most important in controlling the observed increase in the Gd anomalies along the course of the Moselle river. Furthermore, the calculations of Gd anomalies using different approaches (Table 1) would result in different longitudinal patterns of Gd contamination along the Moselle River. For example, the threshold of 1.8 for a Gd anthropogenic anomaly is already exceeded at Le Pont Jean (rkm 9.5) when using Eq. (6), but only between Millery (rkm 202) and Malling (rkm 293) when using Eq. (4).

For the Moselle River tributaries (Table SM4 of the Supplementary Materials), the gadolinium positive anomaly is only clear in REEs patterns of the Madon River (Ma) and of tributaries of the Moselle River downstream of Nancy (Gd/Gd*: 1.8–12.7), except for the Orne River (Gd/Gd*: 1.4) (Table SM6 of the Supplementary Materials). Positive gadolinium anomalies are particularly noticeable for the Rupt-de-Mad and Fensch rivers, with values of 6.6 and 12.7, respectively. The Rupt-de-Mad River is a small river (54 km long), with a small average flow (3.6 m^3/s), and its catchment drains a population of approximately 5400 inhabitants. In relation to its length, the Rupt-de-Mad River has many WWTPs (nine WWTPs, representing a total of 5100 person equivalent) that have simple treatment processes (pretreatment, sand filter, infiltration, even constructed wetland). The Fensch River sampling point is located downstream of a WWTP discharge, this WWTP treats the sewage water of the whole Fensch valley (17 townships, 100,000 person equivalent).

3.4. REEs fluxes

Total REEs (sum of all REEs) fluxes were estimated at different sampling points (i.e., where flow rate values were available) (Table 2). It should be noted that during the sampling periods, average flow conditions were observed for all streams. The "Golbey" (rkm 78) and "Millery" (rkm 202) samples display the most important REEs fluxes (768. and 1083.60 $\times 10^{-3}$ $kg.d^{-1}$). The "Golbey" sampling point is located just downstream of the first large community along the Moselle River (Epinal, at rkm 71). The "Millery" point is located downstream of the Moselle River and the Meurthe River confluence (north of Nancy). The Meurthe River is particularly loaded with minerals due to the presence of quarries along its course. Moreover, the Moselle River receives effluents from the Grand Nancy WWTP, which could explain the increase in Gd_{anth} flux between Gondreville and Millery. Globally,

Table 1
Gadolinium anomaly calculations along the Moselle River course using different equations. Gd^* and Gd_{anth} in ppt calculated with Dy and Nd. Gradient from the lowest (dark blue) to highest (dark red) Gd anomaly.

	rkm	Gd/Gd* (Dy & Nd)	Gd/Gd* (Sm & Tb)	Gd/Gd* (Eu & Nd)	Gd/Gd* (Sm & Nd)	Gd*	Gd_{anth}	$\%Gd_{anth}$
Source		1.6	1.5	0.9	0.6	-	-	-
Les Sources	1.17	1.5	1.2	1.0	0.6	-	-	-
Bussang	3.1	1.4	1.2	1.2	0.5	-	-	-
St-Maurice	7.8	1.5	1.2	1.0	0.6	-	-	-
Le Pont Jean	9.5	1.8	1.6	1.2	0.8	11.5	9.3	44.5
Fresse /Mos.	11.4	1.9	1.5	1.2	0.8	11.5	10.7	48.1
Le Thillot	14.3	2.3	2.0	1.4	1.0	11.8	13.8	55.6
Ramonchamp	18.9	2.4	2.0	1.5	1.1	12.0	16.6	58.1
Ferdrupt	21.7	2.0	1.7	1.4	0.8	12.1	11.6	48.9
Rupt	27.7	1.9	1.7	1.3	0.8	11.1	10.2	47.9
Les Meix	29.9	2.7	2.3	1.8	1.2	11.6	20.3	63.5
Vecoux	36.9	1.9	1.7	1.3	0.8	11.8	11.1	48.5
Eloyes	53.3	1.8	1.4	1.2	0.7	18.5	14.2	43.4
Arches	62.3	1.8	1.4	1.2	0.8	16.6	14.0	45.7
Golbey	78	1.8	1.4	1.1	0.8	16.3	12.4	43.3
Chavelot	81	2.1	1.7	1.4	1.0	14.4	16.2	53.0
Châtel	93	2.1	1.8	1.3	1.0	13.2	14.2	51.8
Portieux	98.6	2.2	2.0	1.3	1.0	11.4	14.1	55.1
Charmes	103.5	2.2	1.9	1.3	1.1	11.6	14.0	54.6
Bainville	114	2.4	2.0	1.4	1.3	10.2	14.2	58.1
Bayon	122	2.4	2.1	1.5	1.3	9.6	13.6	58.5
Velle / Mos.	129	2.4	2.1	1.4	1.4	9.0	12.7	58.6
Tonnoy	133	2.5	2.1	1.5	1.3	9.0	13.2	59.6
Flavigny	140	2.5	2.1	1.4	1.3	9.4	14.2	60.3
Messein	144	2.4	2.3	1.4	1.2	8.2	11.9	59.0
Maron	154	2.3	2.1	1.5	1.1	6.7	9.1	57.4
Pierre	166	2.5	2.1	1.4	1.1	6.1	9.3	60.4
Gondreville	176	2.9	2.5	1.7	1.2	5.4	10.3	65.5
Liverdun	189	2.7	2.6	1.6	1.4	4.5	7.7	63.2
Millery	202	4.4	3.9	2.4	2.5	5.5	18.6	77.2
Dieulouard	209	8.7	9.2	3.4	4.0	2.6	19.8	88.5
Corny	235	5.0	5.3	2.1	2.9	2.7	10.7	80.0
Ay	266	7.6	8.5	4.0	2.6	2.6	17.5	86.9
Bousse	268	7.9	7.4	3.8	2.3	2.8	19.4	87.3
Malling	293	8.4	9.1	3.5	5.4	2.5	18.2	88.1

Table 2
REEs fluxes along the Moselle River course (in 10^{-3} kg.d^{-1}).

	Flow m^3/s	Drained area km^2	Cumulated population millions	Gd	Gd_{anth}	LREEs	MREEs	HREEs	REEs
				10^{-3} kg.d^{-1}					
Fresse	1.05	71	0.0045	2.00	0.96	21.21	4.53	2.80	28.54
Rupt	2.67	152	0.0142	4.910	2.4	45.32	10.80	7.50	63.50
Vecoux	10.8	589	0.0151	21.14	10.32	197.27	46.33	32.62	276.23
Golbey	22.6	1217	0.134	56.10	24.27	541.22	123.5	103.20	768.00
Châtel	22.3	1491	0.163	52.88	27.40	434.14	104.51	86.4	625.10
Velle	27.4	1975	0.180	51.27	30.00	383.36	92.42	77.86	553.65
Gondreville	37.3	3338	0.247	50.85	33.33	321.43	88.92	65.48	475.82
Millery	69.5	6830	0.690	144.69	109.46	580.71	204.05	127.4	912.16

as expected, the Gd_{anth} flux increases with the population expansion along the Moselle River: a linear correlation (at a significance level of 5%) was obtained between the Gd_{anth} flux and the cumulated population in the watershed between the source and Millery (coefficient of determination = 0.99) (Fig. 6). The anthropogenic REEs (AREEs) pool represented between 3 and 24% of the REEs flux, and this proportion increased from upstream to downstream along with the cumulative population. These results agREEs with those of Hissler et al. (2014) for the Alzette River basin under similar flow conditions. Some comparisons of AREEs fluxes could be made with other rivers despite the inherent uncertainties in flux calculations based on a single sampling. For the Moselle River catchment, the specific Gd_{anth} flux has been estimated to be between 1.4 and 2.0 × 10^{-4} kg.d^{-1}.km^{-2}. In comparison, AREEs fluxes have been estimated to range from 7.0 × 10^{-5} kg.d^{-1}.km^{-2} (Kulaksız and Bau, 2013, using Eu and Sm to calculate Gd_{anth}) to 1.2 × 10^{-3} kg.d^{-1}.km^{-2} in the Rhine River (Klaver et al., 2014, at Lobith station, using Sm and Tb to calculate Gd_{anth} and including La_{anth}), 1.1 × 10^{-4} kg.d^{-1}.km^{-2} in the Alzette River (Hissler et al., 2015, using Dy and Nd to calculate Gd_{anth}) and 8.0 × 10^{-6} kg.d^{-1}.km^{-2} in the Weser River (Kulaksız and Bau, 2007, using Sm and Tb to calculate Gd_{anth}).

3.5. Potential toxicity due to REEs in the Moselle River watershed

Concentrations of individual lanthanides measured in the French part of the Moselle River watershed are at least thREEs orders of magnitude lower than levels reported to be of potential concern in ecotoxicological studies (González et al., 2015; Galdiero et al., 2019). The sum of all lanthanides, which is usually assumed to share the same mode of action, is also below levels reported to be of potential concern (Romero-Freire et al., 2018). Such comparisons must however be interpreted with the utmost caution considering that the actual ecotoxicity of lanthanides may be underestimated because of our limited knowledge of their speciation in standardized tests (Gonzalez et al., 2014).

In the specific case of Gd, the possible ecotoxicological effects of Gd_{ant} ought to be compared with those of gadoteric acid, or other representative Gd-based MRI contrast agents, rather than with those of inorganic Gd forms. The average concentration of Gd_{ant} was 13.6 ± 3.4 ng/L (arithmetic mean ± 1 standard deviation, n = 30, Table 1) in the Moselle River and ranged from about 2 to 76 ng/L in the Moselle tributaries (Table SM6). These levels are close to, or exceed, the value of 20 ng/L of gadoteric acid reported to slow down the growth of cultured fish cells in laboratory tests (Parant et al., 2019). Parant et al. (2019) also note that the ecotoxicity of gadoteric acid may originate from its chelating structure rather than from the Gd ion itself, confirming that the biological effects of natural and anthropogenic Gd must be evaluated independently. In particular, estimation of anthropogenic Gd anomalies via ICP-MS measurements should be completed by determination of the exact structure of the contrasting agents actually responsible for the observed Gd anomalies (Birka et al., 2016).

Taking into account the difficulties to separate REEs one from another due to their similar chemical and physical properties, the presence of REEs other than Gd in Gd-based contrast agents cannot be excluded (Veiga et al., 2020). Finally, if Gd is largely used for MRI, other REEs are currently investigated to improve the diagnostic sensitivity (Baek et al., 2020). Continued (and possibly continuous) monitoring, especially under low-flow conditions, will be of particular importance given that the anthropogenic Gd load originates from WWTP whose contribution to river flow becomes more important during droughts.

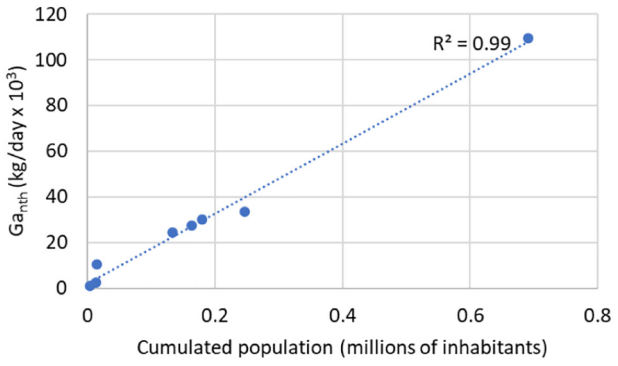

Fig. 6. Relation between the Gd_{anth} flux and the cumulative population.

4. Conclusions

The REEs patterns of headstream waters vary greatly and are strongly affected by substrate geology, with clear negative Ce anomalies, LREEs depletion and HREEs enrichment being the most distinctive characteristics of water flowing on tuff, graywacke and sandstone. On the other hand, a granite substrate imparts a typical concave shape to the REEs profiles (likely linked to the presence of phosphate-based minerals) along with a slight Eu negative anomaly (also linked to basin lithology).

A Ce anomaly is present along the whole Moselle River, although it tends to decrease along the river course in response to changes in geology. LREEs depletion and HREEs enrichment (along with anthropogenic Gd enrichment) are the most distinctive features of REEs profiles downstream of Epinal (rkm 71.2) where the basin geology changes from predominantly crystalline to sedimentary rocks. The corresponding La_{PAAS}/Yb_{PAAS} ratios show a regular decreasing trend along the river course as a function of pH and the increasing predominance of carbonated rocks in the river basin.

Based on calculations using Dy and Nd, the presence of Gd anomalies can be detected at the Moselle River source as well as in some Moselle River headstreams and tributaries. Inputs from WWTPs and decentralized sewage treatment units may account for such anomalies. On the other hand, the use of different calculation methods can shift the appearance of the anthropogenic Gd anomaly in the Moselle River further downstream. Consequently, the choice of threshold values to identify the presence of Gd anomalies must be carefully evaluated against local or basin-scale geological peculiarities, and extrapolation between rivers should

be performed with care. Similar recommendations apply when comparing anthropogenic Gd fluxes among different river basins.

The methodology used for calculating Gd anomalies also influences the subsequent estimation of natural vs. anthropogenic Gd levels and must be accounted for when trying to assess the possible ecotoxicological effects of anthropogenic Gd. In this sense, the use of the Dy- and Nd-based calculation (which tends to maximize Gd anomalies and, hence, Gd anthropogenic concentrations) represents a conservative approach for risk evaluation. Considering that the ecotoxicological effects of Gd-based contrast agents may be linked to their chelating structures rather than the Gd ion itself, routine ICP-MS measurements should however be completed by other techniques to identify the exact structure of the compounds responsible for the observed Gd anomalies.

CRediT authorship contribution statement

Pauline Louis: Investigation, Methodology, Data curation, Writing - original draft. **Abdelkrim Messaoudene:** Investigation. **Hayfa Jrad:** Investigation. **Barakat A. Abdoul-Hamid:** Investigation. **Davide A.L. Vignati:** Formal analysis, Writing - review & editing, Funding acquisition, Supervision. **Marie-Noëlle Pons:** Investigation, Conceptualization, Supervision, Project administration, Funding acquisition, Writing - review & editing.

Declaration of competing interest

The authors declare that they have no known competing financial interests or personal relationships that could have appeared to influence the work reported in this paper.

Acknowledgments

The authors acknowledge the financial support from the National Agency for Research – France (ANR) through the project ANR-16-CE34-0012-001. The authors thank the forest rangers of Moussey and Xoulces (ONF) and B. Pollier (INRAE) for the collection of headstream samples. Loïc Martin and Christophe Hissler are thanked for fruitful discussions on the data and data treatment procedures.

Appendix A. Supplementary data

Supplementary data to this article can be found online at https://doi.org/10.1016/j.scitotenv.2020.140619.

References

Aubert, D., Stille, P., Probst, A., 2001. REEs fractionation during granite weathering and removal by waters and suspended loads: Sr and Nd isotopic evidence. Geochim. Cosmochim. Acta 65, 387–406.

Aubert, D., Stille, P., Probst, A., Gauthier-Lafaye, F., Pourcelot, L., 2002. Characterization and migration of atmospheric REEs in soils and surface waters. Geochim. Cosmochim. Acta 66, 3339–3350.

Baek, A., Kim, H., Yang, J., Choi, G., Kim, M., Cho, A.E., Kim, Y., Kim, S., Sung, B., Yang, B.W., Seo, H., Lee, G.H., Ryom, H.K., Jung, H., Lee, T., Chang, Y., 2020. High-performance hepatobiliary dysprosium contrast agent for ultra-high-field magnetic resonance imaging. J. Ind. Eng. Chem. 85, 297–307.

Bau, M., 1991. Rare-earth element mobility during hydrothermal and metamorphic fluid–rock interaction and the significance of the oxidation state of europium. Chem. Geol. 93, 219–230.

Bau, M., 1999. Scavenging of dissolved yttrium and rare earths by precipitating iron oxyhydroxide: experimental evidence for Ce oxidation, Y-Ho fractionation, and lanthanide tetrad effect. Geochim. Cosmochim. Acta 63, 67–77.

Bau, M., Dulski, P., 1996. Anthropogenic origin of positive gadolinium anomalies in river waters. Earth Planet. Sci. Lett. 143, 245–255.

Bau, M., Knappe, A., Dulski, P., 2006. Anthropogenic gadolinium as a micropollutant in river waters in Pennsylvania and in Lake Erie, northeastern United States. Chem. Erde - Geochem. 66, 143–152. https://doi.org/10.1016/j.chemer.2006.01.002.

Birka, M., Wehe, C.A., Hachmöller, O., Sperling, M., Karst, U., 2016. Tracing gadolinium-based contrast agents from surface water to drinking water by means of speciation analysis. J. Chromatogr. A 1440, 105–111.

Byrne, R.H., Kim, K.-H., 1990. Rare earth element scavenging in seawater. Geochim. Cosmochim. Acta 54, 2645–2656.

Chazot, A., Barrat, J.A., Jomaah, R., Ognard, J., Ben Salem, D. 2020. Gaha, M., Brain MRIs makeup the bulk of the gadolinium footprint in medical imaging. J. Neuroradiol. 47, 259–265.

Czoch, D., 2019. Pharmacokinetics of gadolinium-based contrast agents. Radiologe 59, 408–412.

De Baar, H.J.W., German, C.R., Elderfield, H., Van Gaans, P., 1988. Rare earth element distributions in anoxic waters of the Cariaco Trench. Geochim. Cosmochim. Acta 52, 1203–1219.

Deal, S.C., Gilliam, J.W., Skaggs, R.W., Kohyha, K.D., 1986. Prediction of nitrogen and phosphorus losses as related to agricultural drainage system design. Agric. Ecosyst. Environ. 18, 37–51.

Driscoll, C.T., Lawrence, G.B., Bulger, A.J., Butler, T.J., Cronan, C.S., Eagar, C., Lambert, K.F., Likens, G.E., Stoddard, J.L., Weathers, K.C., 2001. Acidic deposition in the northeastern United States: sources and inputs, ecosystem effects, and management strategies. BioScience 51, 180–198.

Du, X., Graedel, T.E., 2011. Global in-use stocks of the rare earth elements: a first estimate. Environ. Sci. Technol. 45, 4096–4101.

Elbaz-Poulichet, F., Seidel, J.-L., Othoniel, C., 2002. Occurrence of an anthropogenic gadolinium anomaly in river and coastal waters of southern France. Water Res. 36, 1102–1105.

Elderfield, H., Upstill-Goddard, R., Sholkovitz, E.R., 1990. The rare earth elements in rivers, estuaries, and coastal seas and their significance to the composition of ocean waters. Geochim. Cosmochim. Acta 54, 971–991.

Galdiero, E., Carotenuto, R., Siciliano, A., Libralato, G., Race, M., Lofrano, G., Fabbricino, M., Guida, M., 2019. Cerium and erbium effects on *Daphnia magna* generations: a multiple endpoints approach. Environ. Pollut. 254, 112985.

Gasanov, A.A., Naumov, A.V., Yurasova, O.V., Petrov, I.M., Litvinova, T.E., 2018. Certain tendencies in the Rare-Earth-Element world market and prospects of Russia. Russ. J. Non-Ferr. Met. 59, 502–511.

German, C.R., Elderfield, H., 1989. Application of the Ce anomaly as a paleoredox indicator: the ground rules. Paleoceanography 5, 823–833.

Gonzalez, V., Vignati, D.A.L., Leyval, C., Giamberini, L., 2014. Environmental fate and ecotoxicity of lanthanides: are they a uniform group beyond chemistry? Environ. Int. 71, 148–157.

González, V., Vignati, D.A.L., Pons, M.-N., Montarges-Pelletier, E., Bojic, C., Giamberini, L., 2015. Lanthanide ecotoxicity: first attempt to measure environmental risk for aquatic organisms. Environ. Pollut. 199, 139–147.

Hannigan, R.E., Sholkovitz, E.R., 2001. The development of middle rare earth element enrichments in freshwaters: weathering of phosphate minerals. Chem. Geol. 175, 495–508.

Haxel, G., 2002. Rare Earth Elements: Critical Resources for High Technology. U.S. Department of the Interior, U.S. Geological Survey.

Henze, M., Harremoës, P., la Cour Jansen, J., Arvin, E., 2002. Wastewater Treatment, Biological and Chemical Processes. 3rd edition. Springer, Heidelberg, Germany.

Hissler, C., Stille, P., Guignard, C., Iffly, J.F., Pfister, L., 2014. Rare earth elements as hydrological tracers of anthropogenic and critical zone contributions: a case study at the Alzette River basin scale. Procedia Earth Planet. Sci. 10, 349–352.

Hissler, C., Hostache, R., Iffly, J.F., Pfister, L., Stille, P., 2015. Anthropogenic rare earth element fluxes into floodplains: coupling between geochemical monitoring and hydrodynamic sediment transport modelling. Compt. Rendus Geosci. 347, 294–303.

Hissler, C., Stille, P., Iffly, J.F., Guignard, C., Chabaux, F., Pfister, L., 2016. Origin and dynamics of rare earth elements during flood events in contaminated river basins: Sr–Nd–Pb isotopic evidence. Environ. Sci. Technol. 50, 4624–4631.

Humphries, M., 2010. Rare Earth Elements: The Global Supply Chain. DIANE Publishing.

Inoue, K., Fukushi, M., Furukawa, A., Sahoob, S.K., Veerasamy, N., Ichimura, K., Kasahara, S., Ichihara, M., Tsukada, M., Torii, M., Mizaghuchi, M., Taguchi, Y., Nakazawa, S., 2020. Impact on gadolinium anomaly in river waters in Tokyo related to the increased number of MRI devices in use. Mar. Pollut. Bull. 154, 111148.

Johannesson, K.H., Lyons, W.B., 1994. The rare earth element geochemistry of Mono Lake water and the importance of carbonate complexing. Limnol. Oceanogr. 39, 1141–1154.

Kim, I., Kim, S.H., Kim, G., 2020. Anthropogenic gadolinium in lakes and rivers near metrocities in Korea. Environ Sci Process Impacts 22, 144–151.

Klaver, G., Verheul, M., Bakker, I., Petelet-Giraud, E., Négrel, P., 2014. Anthropogenic Rare Earth Element in rivers: gadolinium and lanthanum. Partitioning between the dissolved and particulate phases in the Rhine River and spatial propagation through the Rhine-Meuse Delta (the Netherlands). Appl. Geochem. 47, 186–197.

Knappe, A., Möller, P., Dulski, P., Pekdeger, A., 2005. Positive gadolinium anomaly in surface water and ground water of the urban area Berlin, Germany. Chem. Erde - Geochem. 65, 167–189.

Kulaksız, S., Bau, M., 2007. Contrasting behaviour of anthropogenic gadolinium and natural rare earth elements in estuaries and the gadolinium input into the North Sea. Earth Planet. Sci. Lett. 260, 361–371.

Kulaksız, S., Bau, M., 2011a. Anthropogenic gadolinium as a microcontaminant in tap water used as drinking water in urban areas and megacities. Appl. Geochem. 26, 1877–1885.

Kulaksız, S., Bau, M., 2011b. Rare earth elements in the Rhine River, Germany: first case of anthropogenic lanthanum as a dissolved microcontaminant in the hydrosphere. Environ. Int. 37, 973–979.

Kulaksız, S., Bau, M., 2013. Anthropogenic dissolved and colloid/nanoparticle-bound samarium, lanthanum and gadolinium in the Rhine River and the impending destruction of the natural rare earth element distribution in rivers. Earth Planet. Sci. Lett. 362, 43–50.

Kümmerer, K., Helmers, E., 2000. Hospital effluents as a source of gadolinium in the aquatic environment. Environ. Sci. Technol. 34, 573–577.

Lerat-Hardy, A., Coynel, A., Dutruch, L., Pereto, C., Bossy, C., Gil-Diaz, T., Capdeville, M.-J., Blanc, G., Schäfer, J., 2019. Rare Earth Element fluxes over 15 years into a major European Estuary (Garonne-Gironde, SW France): hospital effluents as a source of increasing gadolinium anomalies. Sci. Total Environ. 656, 409–420.

Leybourne, M.I., Goodfellow, W.D., Boyle, D.R., Hall, G.M., 2000. Rapid development of negative Ce anomalies in surface waters and contrasting REEs patterns in groundwaters associated with Zn–Pb massive sulphide deposits. Appl. Geochem. 15, 695–723.

McLennan, S.M., 1989. Rare earth elements in sedimentary rocks; influence of provenance and sedimentary processes. Rev. Mineral. Geochem. 21, 169–200.

Merschel, G., Bau, M., Baldewein, L., Dantas, E.L., Walde, D., Bühn, B., 2015. Tracing and tracking wastewater-derived substances in freshwater lakes and reservoirs: anthropogenic gadolinium and geogenic REEs in Lake Paranoá, Brasilia. Compt. Rendus Geosci. 347, 284–293.

Möller, P., Dulski, P., Bau, M., Knappe, A., Pekdeger, A., Sommer-von Jarmersted, C., 2000. Anthropogenic gadolinium as a conservative tracer in hydrology. J. Geochem. Explor. 69–70, 409–414.

Möller, P., Knappe, A., Dulski, P., 2014. Seasonal variations of rare earths and yttrium distribution in the lowland Havel River, Germany, by agricultural fertilization and effluents of sewage treatment plants. Appl. Geochem. 41, 62–72.

Nédeltcheva, T., Piedallu, C., Gégout, J.C., Boudot, J.P., Angeli, N., Dambrine, E., 2006a. Environmental factors influencing streamwater composition on sandstone (Vosges Mountains). Ann. For. Sci. 63, 369–376.

Nédeltcheva, T., Piedallu, C., Gégout, J.-C., Stussi, J.M., Boudot, J.P., Angeli, N., Dambrine, E., 2006b. Influence of granite mineralogy, rainfall, vegetation and relief on stream water chemistry (Vosges Mountains, North-Eastern France). Chem. Geol. 231, 1–15.

Nozaki, Y., Lerche, D., Alibo, D.S., Tsutsumi, M., 2000. Dissolved indium and rare earth elements in thREEs Japanese rivers and Tokyo Bay: evidence for anthropogenic Gd and In. Geochim. Cosmochim. Acta 64, 3975–3982.

Olivarez, A.M., Owen, R.M., 1991. The europium anomaly of seawater: implications for fluvial versus hydrothermal REEs inputs to the oceans. Chem. Geol. 92, 317–328.

Parant, M., Sohm, B., Flayac, J., Perrat, E., Chuburu, F., Cadiou, C., Rosin, C., Cossu-Leguille, C., 2019. Impact of gadolinium-based contrast agents on the growth of fish cells lines. Ecotox. Environ. Safe. 182, 109385.

Pereto, C., Coynel, A., Lerat-Hardy, A., Gourves, P.-Y., Schäfer, J., Baudrimont, M., 2020. *Corbicula fluminea*: A sentinel species for urban Rare Earth Element origin. Sci. Total Environ. 732, 138552.

Perrat, E., Parant, M., Py, J.-S., Rosin, C., Cossu-Leguille, C., 2017. Bioaccumulation of gadolinium in freshwater bivalves. Environ. Sci. Pollut. Res. 24, 12405–12415.

Rabiet, M., Brissaud, F., Seidel, J.L., Pistre, S., Elbaz-Poulichet, F., 2009. Positive gadolinium anomalies in wastewater treatment plant effluents and aquatic environment in the Hérault watershed (south France). Chemosphere 75, 1057–1064.

Romero-Freire, A., Minguez, L., Pelletier, M., Cayer, A., Caillet, C., Devin, S., Gross, E.M., Guérold, F., Pain-Devin, S., Vignati, D.A.L., Giamberini, L., 2018. Assessment of baseline ecotoxicity of sediments from a prospective mining area enriched in light rare earth elements. Sci. Total Environ. 612, 831–839.

Schmidt, K., Bau, M., Merschel, G., Tepe, N., 2019. Anthropogenic gadolinium in tap water and in tap water-based beverages from fast-food franchises in six major cities in Germany. Sci. Total Environ. 687, 1401–1408.

Sholkovitz, E.R., 1992. Chemical evolution of rare earth elements: fractionation between colloidal and solution phases of filtered river water. Earth Planet. Sci. Lett. 114, 77–84.

Sholkovitz, E.R., 1995. The aquatic chemistry of rare earth elements in rivers and estuaries. Aquat. Geochem. 1, 1–34.

Steinhauser, G., 2008. Cleaner production in the Solvay process: general strategies and recent developments. J. Clean. Prod. 16, 833–841.

Stille, P., Steinmann, M., Pierret, M.-C., Gauthier-Lafaye, F., Chabaux, F., Viville, D., Pourcelot, L., Matera, V., Aouad, G., Aubert, D., 2006. The impact of vegetation on REEs fractionation in stream waters of a small forested catchment (the Strengbach case). Geochim. Cosmochim. Acta 70, 3217–3230. https://doi.org/10.1016/j.gca.2006.04.028.

Tepe, N., Romero, M., Bau, M., 2014. High-technology metals as emerging contaminants: strong increase of anthropogenic gadolinium levels in tap water of Berlin, Germany, from 2009 to 2012. Appl. Geochem. 45, 191–197.

Tricca, A., Stille, P., Steinmann, M., Kiefel, B., Samuel, J., Eikenberg, J., 1999. Rare earth elements and Sr and Nd isotopic compositions of dissolved and suspended loads from small river systems in the Vosges mountains (France), the river Rhine and groundwater. Chem. Geol. 160, 139–158.

Veiga, M., Mattiazzi, P., de Gois, J.S., Nascimento, P.C., Borges, D.L.G., Bohrer, D., 2020. Presence of other rare earth metals in gadolinium-based contrast agents. Talanta 216, 120940.

Verplanck, P.L., Taylor, H.E., Nordstrom, D.K., Barber, L.B., 2005. Aqueous stability of gadolinium in surface waters receiving sewage treatment plant effluent, Boulder Creek, Colorado. Environ. Sci. Technol. 39, 6923–6929.

Verplanck, P.L., Furlong, E.T., Gray, J.L., Phillips, P.J., Wolf, R.E., Esposito, K., 2010. Evaluating the behavior of gadolinium and other rare earth elements through large metropolitan sewage treatment plants. Environ. Sci. Technol. 44, 3876–3882.

Yeghicheyan, D., Aubert, D., Bouhnik-Le Coz, M., Chmeleff, J., Delpoux, S., Djouraev, I., Granier, G., Lacan, F., Piro, J., Rousseau, T., Cloquet, C., Marquet, A., Menniti, C., Pradoux, C., Freydier, R., Vieira da Silva-Filho, E., Suchorski, K., 2019. A new interlaboratory characterisation of silicon, rare earth elements and twenty-two other trace element concentrations in the Natural River Water Certified Reference Material SLRS-6 (NRC - CNRC). Geostand. Geoanal. Res. 43, 475–496.